Lithium-mediated Mechanochemical Cyclodehydrogenation

Kanna Fujishiro,[†] Yuta Morinaka,[#] Yohei Ono,[#] Tsuyoshi Tanaka,[♭] Lawrence T. Scott,[¶] Hideto Ito,[†,*] and Kenichiro Itami*[,†,‡]

[†] Department of Chemistry, Graduate School of Science, Nagoya University, Nagoya 464-8602, Japan. [‡] Institute of Transformative Bio-Molecules (WPI-ITbM), Nagoya University, Nagoya 464-8602, Japan. [#] Tokyo Research Center, Organic Materials Research Laboratory, Tosoh Corporation, 2743-1 Hayakawa, Ayase, Kanagawa 252-1123, Japan. [♭] Tosoh Corporation, 3-8-2 Shiba, Minato-ku, Tokyo 105-8623, Japan. [¶] Department of Chemistry, University of Nevada, Reno, Nevada 89557-0216, United States.

ABSTRACT: Cyclodehydrogenation is an essential synthetic method for the preparation of polycyclic aromatic hydrocarbons, polycyclic heteroaromatic compounds, and nanographenes. Among the many examples, anionic cyclodehydrogenation using potassium(0) has attracted synthetic chemists because of its irreplaceable reactivity and utility in obtaining rylene structures from binaphthyl derivatives. However, existing methods are difficult to use in terms of practicality, pyrophoricity, and lack of scalability and applicability. Herein, we report the development of a lithium(0)-mediated mechanochemical anionic cyclodehydrogenation reaction for the first time. This reaction could be easily performed using a conventional and easy-to-handle lithium(0) wire at room temperature, even under air, and the reaction of 1,1′-binaphthyl is complete within 30 min to afford perylene in 94% yield. Using this novel and user-friendly protocol, we investigated substrate scope, reaction mechanism, and gram-scale synthesis. As a result, remarkable applicability and practicality over previous methods, as well as limitations, were comprehensively studied by computational studies and NMR analysis. Furthermore, we demonstrated two-, three-, and five-fold cyclodehydrogenations for the synthesis of novel nanographenes. In particular, quinterrylene ([5]rylene or pentarylene), the longest non-substituted molecular rylene, was synthesized for the first time.

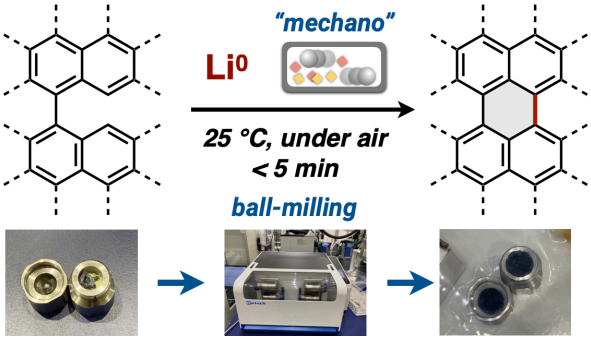

Introduction

Lithium metal possesses the lowest reduction electrode potential (−3.04 V vs. standard hydrogen electrode (SHE)) compared to other metals, and its lightness and high specific capacity (3.86 Ah g^{-1}) allow us to utilize lithium as a high-voltage and high-capacity Li-ion battery (Figure 1A).[1] Lithium is a key reactive main group metal element in organic chemistry, used in the preparation of organolithium reagents and lithium alkoxides, as well as general reduction reactions such as Birch reduction.[2] In these reactions, the bulk of Li (wire, shot, granule, or dispersion) itself never dissolves in aprotic organic solvents, but it gradually reacts with substrates (alkyl/aryl halides, alcohols, amines, and other electrophiles) on the solid-liquid interface, thus forming organolithium species that could dissolve in organic solvents. However, regardless of the highest reduction potential, Li shows the lowest reactivity among other alkali metals in the solution state, which is a common phenomenon in organic chemistry. The reason for the actual low reactivity is rationalized by the higher atomization energy (ΔH_{atom} = 159 kJ/mol) of Li, where ΔH_{atom} is the enthalpy change in breaking all of a compound's bonds (metal bonds in Li) into separated single atoms. Comparatively, Na and K, with larger atomic radii than Li, have 107 and 89 kJ/mol of ΔH_{atom}, respectively (Figure 1A).[3] In other words, the potential highest reducing ability of Li gets masked in the heterogeneous solution state reactions.

An example of the lower reactivity of Li in organic synthesis is the alkali-metal-mediated cyclodehydrogenation[4,5] of polyarylenes for the synthesis of polycyclic aromatic hydrocarbons (PAHs), mainly including rylene substructures. Since Scholl and Clar first explored syntheses of PAHs in the 1900s,[5] PAHs including nanocarbons have received tremendous attention in organic chemistry, materials science, biology, and astrochemistry.[6] Despite recent advances in molecular nanocarbon synthesis[7] via cross-coupling reactions, the Diels–Alder reaction, and on-surface synthesis for preparing nonclassical nanocarbons such as warped nanographenes[8,4d] and graphene nanoribbons,[9] the final synthetic step for stitching (graphitizing or planarizing) polyarylenes continues to rely heavily on cyclodehydrogenation reactions. Among them, the Scholl reaction,[9] which proceeds in the presence of oxidants such as $FeCl_3$, $AlCl_3$, or DDQ/TfOH (DDQ = 2,3-dichloro-5,6-dicyano-1,4-benzoquinone, TfOH = trifluoromethanesulfonic acid), is undoubtedly one of the most useful cyclodehydrogenation reactions and plays a central role in the synthesis of polycyclic aromatics. However, successful examples of the Scholl reaction are mostly limited to six-membered ring closures of electron-rich *ortho*-terphenyls and structurally constrained helicenes. In other cases, the reaction often results in undesired aromatic rearrangements,[10,11] decomposition, and chlorination (Figure 1B).[4] For example, the $AlCl_3$/NaCl-promoted Scholl reaction does not perform well for the cyclodehydrogenation of 1,1′-binaphthyl, yielding only 15% of perylene.[5] TfOH-promoted

reaction of 1,1′-binaphthyl is known to give benzofluoranthene, 2,2′-binaphthyl, and 1,2′-binaphthyl through a 1,2-aryl shifts.[11] Scholl reaction of electron-deficient pyridine derivatives is also ineffective, and introducing electron-donating substituents such as *t*-Bu and OMe groups is required for the reaction to proceed.[12] For achieving such difficult cyclodehydrogenation, potassium(0)- or potassium-intercalated carbon (KC_8)-mediated anionic cyclodehydrogenation is known to be an alternative but irreplaceable method.[13] While earlier examples were not reported in detail,[14] in 2010, Scott revisited to developed a cyclodehydrogenation of 1,1′-binaphthyl using potassium metal in THF and reported the detailed reaction profile and mechanism.[13a] The reaction is typically carried out in a pressure vessel with degassed and dehydrated THF at 85 °C under an inert gas atmosphere, and perylene is quantitatively obtained after heating for 12 h. Since then, this cyclodehydrogenation method has been regarded as an alternative method for obtaining rylene structures[13b–f] and electron-deficient polyaromatics (Figure 1C).[15] However, compared to the established Scholl reactions, this method has not been widely employed due to the lower yields of products, narrow substrate scope, small scalability, and poor handleability caused by the pyrophoric nature of potassium(0). In addition, a heterogeneous reaction system with metallic potassium in THF or toluene disfavors the synthesis of planar and poorly soluble molecular nanocarbons.

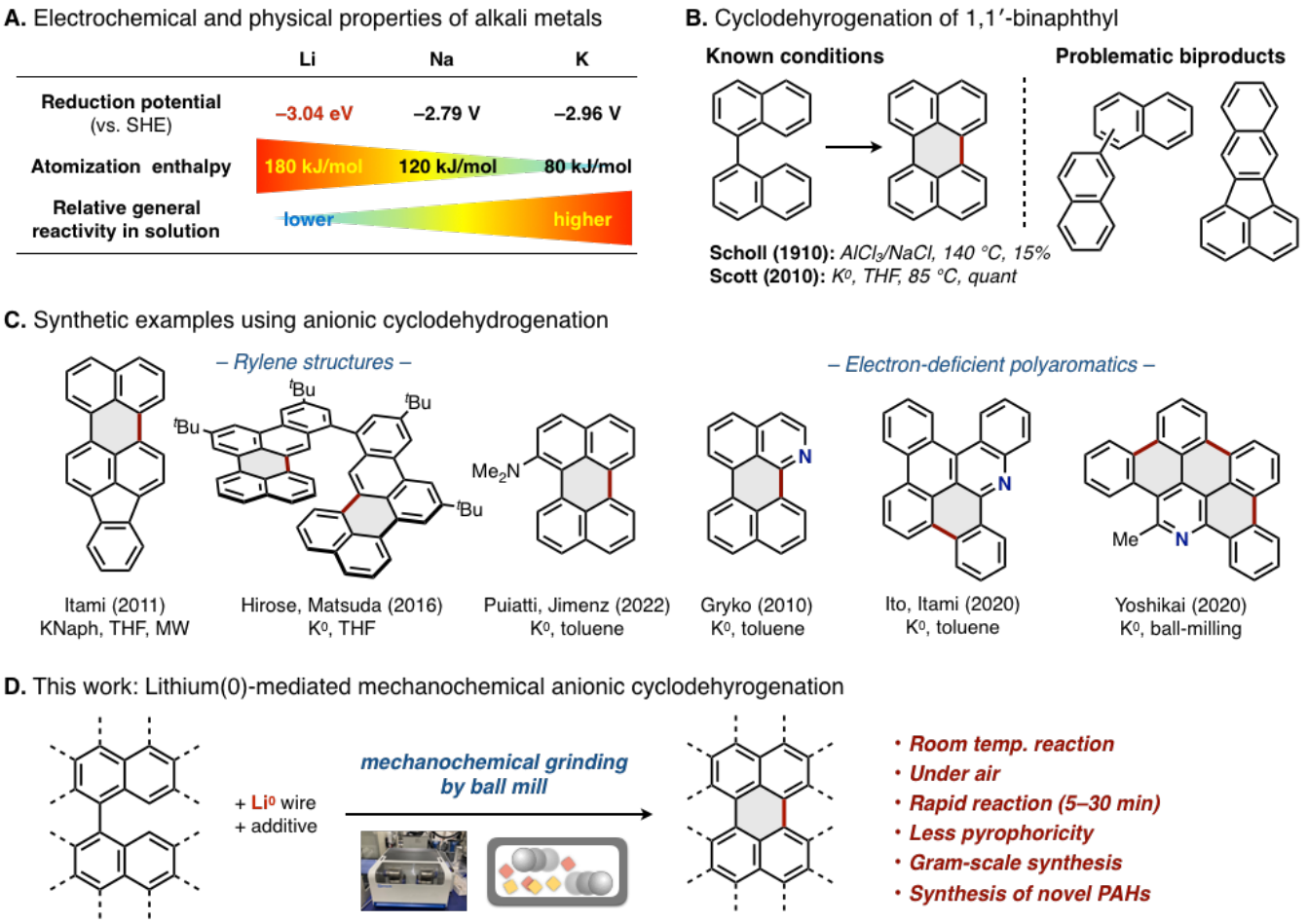

Figure 1. (**A**) Properties of alkali metals, (**B**) cyclodehydrogenation of 1,1′-binaphthyl, (**C**) alkali metal-mediated anionic cyclodehydrogenation, and (**D**) lithium(0)-mediated mechanochemical anionic cyclodehydrogenation (this work).

Herein, we report a lithium(0)-mediated mechanochemical cyclodehydrogenation reaction that exploits the potentially high reducing ability of lithium in the solid-state ball-milling reaction (Figure 1D). Directly mixing pieces of easy-to-handle lithium(0) wire and various binaphthyls with stainless balls in a stainless-steel jar followed by rapid shaking by a ball-milling machine at room temperature enables the synthesis of various rylene-type PAHs and electron-deficient PAHs in a short reaction time. Using this methodology, we not only improved the yield of known compounds and achieved gram-scale synthesis but also succeeded in synthesizing unprecedented molecular nanocarbons.

Results and Discussion

Modification of reaction conditions

Our interest in developing mechanochemical dehydrogenations originated from our previous campaign in developing new synthetic methodologies for PAHs, nanographenes, and polycyclic heteroaromatics,[16,17] the mechanochemical synthesis of fullerene dimers by Komatsu,[18] and a series of recent marked developments in mechanochemical synthesis.[19,20] We hypothesized that the use of bulk lithium(0) as a reducing agent for solid-state mechanochemical cyclodehydrogenation would have various synthetic advantages for nanocarbon synthesis: i) lithium(0) has the highest reducing ability (the lowest reduction potential) in metals; ii) neither the precursors

nor the PAH products are required to dissolve in organic solvents; iii) handling of lithium(0) (washing, cutting, weighing, adding, removing, and quenching) is easier and safer than sodium(0) and potassium(0), even under air; and iv) a solid-state mechanochemical mixing is expected to form a minute lithium-substrate cluster to enhance the efficient lithium-to-substrate electron transfer, which is slow in the diluted solution-state due to the high atomization enthalpy of Li.

First, we optimized reaction conditions for anionic mechanochemical cyclodehydrogenation of 1,1′-binaphthyl (**1a**, 0.20 mmol, 1.0 eq.) using various metals, additives, and reaction temperatures. We discovered that the use of Li wire pieces (6.0 eq.), THF (12 eq.), and a 7-mm diameter stainless ball in a 1.5-mL volume stainless jar at room temperature (25 °C) under air with mixing by ball milling at a rate of 30 Hz (1800 rpm) for 30 min efficiently afforded perylene (**2a**) in 94% isolated yield (Table 1, entry 1). While the reaction did not complete within 1 min (entry 2), it was remarkable that the reaction was almost complete in 5 min (entry 3), and extension of the reaction time rarely affected the yield. The use of 3 eq. of Li also resulted in a slight decrease in yield (81%, entry 4). The use of 6 eq. of Li (8.3 mg, standard conditions) was more appropriate than the use of 3 eq. Li for the 0.20 mmol-scale reaction in terms of yield, reaction reproducibility, easy handleability, and mixing efficiency, and showed a dependence on the total weight/volume of reaction contents and reaction vessel volume. Decreasing the amount of THF or the absence of THF significantly decreased the yield to 62% and 43%, respectively (entries 5 and 6), whereas using an excess amount of THF (30 eq.) promoted the reaction (entry 7). Notably, adding small amounts of solvent is known to be effective in promoting the mechanochemical reactions, known as liquid-assisted grinding (LAG).[21]

Table 1. Screening and optimization of reaction conditions for lithium(0)-medicated mechanochemical anionic cyclodehydrogenation of 1,1′-binaphthyl (**1a**).

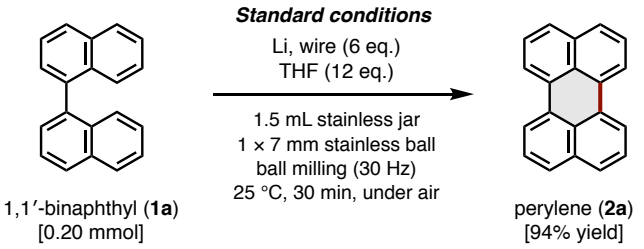

Entry	Deviation from the standard conditions	Yield
1	None	94%
2	Reaction time: 1 min	9%
3	Reaction time: 5 min	91%
4	Li (3 eq.) instead of Li (6 eq.)	81%
5	THF (6 eq.) instead of THF (12 eq.)	62%
6	w/o THF	43%
7	THF (30 eq.) instead of THF (12 eq.)	95%
8	NEt_3 (12 eq.) instead of THF	94%
9	TMEDA (12 eq.) instead of THF	95%
10	Et_2O (12 eq.) instead of THF	88%
11	Naphthalene (1.0 eq.) instead of THF	70%
12	DMAN (1.0 eq.) instead of THF	75%
13	K (6 eq.) instead of Li (6eq.)	49%
14	Na (6 eq.) instead of Li (6 eq.)	28%
15[a]	K (30 eq.), THF, 85 °C, under argon, 12 h	quant
16[b]	Li (30 eq.), THF (4.0 mL), 25 °C, 2 h	0%
17[b]	Li (30 eq.), THF (4.0 mL), 50 °C, 2 h	0.03%

The reactions were quenched with 0.25 M I_2 in THF after the indicated reaction times. [a] Sealed tube instead of ball-milling. Experimental data are presented in ref. 13a. [b] The reactions were carried out in a Schlenk tube with a stirring bar under argon by mixing with a magnetic stirrer in an oil bath.

The parameter of η (the ratio of total liquid volume to the total weight of other solid sample, μL/mg)[21c] of each condition are follows: η = 3.2 μL/mg (entry 1), 3.5 μL/mg (entry 4), 1.6 μL/mg (entry 5), 0.0 μL/mg (entry 6), and 8.1 μL/mg (entry 7). These values indicate that the current reactions with THF additive are slurry reactions (η = ca. 1–10 μL/mg) rather than LAG reactions (LAG = ca. 0.1 μL/mg). Other additives, such as NEt_3, *N,N,N′,N′,*-tetramethylethylenediamine (TMEDA), Et_2O, naphthalene, and 1-(*N,N*-dimethylamino)naphthalene (DMAN), worked well as additives instead of THF, which can also potentially modulate the reactivity of Li for various substrates (entries 8–12). It is also interesting that solid additives such as naphthalene and DMAN slightly promoted the reaction compared to the lithium(0)-alone reaction (entry 6 vs. entries 11 and 12). When alkali metals such as K and Na were employed instead of Li, **1a** was not fully consumed, and the yields of **2a** dropped to 49% and 28%, respectively (entries 13 and 14). This is in stark contrast to a previous report by Scott, who demonstrated the same reaction with highly pyrophoric K in a THF solution under pressurized and heated conditions (entry 15).[13a] The solution-state reaction with a Li wire did not proceed at all at 25 °C or 50 °C (entries 16 and 17). The observed higher reactivity in the solid-state reaction and lower reactivity in the solution-state reaction are considered to correlate with the high reducing ability of lithium and high atomization energy (ΔH_{atom}); thus, the potential high reduction capacity of Li was successfully achieved in the solid-state reaction.

Substrate scope and limitation

With a highly efficient, easy-to-handle mechanochemical reaction in hand, we explored the substrate scope of anionic cyclodehydrogenation of various binaphthyl analogs, particularly by testing unprecedented and poorly soluble substrates (Figure 2). 4,4'-Diphenyl-1,1'-binaphthalene (**1b**), 9-(naphthalen-1-yl)phenanthrene (**1c**), and 6-(naphthalen-1-yl)chrysene (**1d**) were efficiently transformed to substituted perylene **2b** and π-extended perylenes **2c** and **2d** in high yields (92%, 88%, and 82%, respectively). Substrates such as 9,9'-biphenanthrene (**1e**) and 6-(phenanthren-9-yl)chrysene (**1f**) were almost completely consumed, but the π-extended perylenes **2e** and **2f** were easily decomposed in air due to the presence of reactive *bay*-regions,[22] resulting in low isolated yields (18% and 16%) after purification by preparative thin-layer column chromatography (PTLC) on silica gel. On the other hand, 1-(naphthalen-1-yl)pyrene (**1g**) and its isomer 4-(naphthalen-1-yl)pyrene (**1g′**) were found to be suitable substrates for the anionic cyclization, and naphtho[8,1,2-*bcd*]perylene (**2g**) was obtained in 83% and 81% yields using both substrates through small-scale reactions (0.2–0.5 mmol scale). A gram-scale reaction using 1.64 g (5.0 mmol) of **1g** was accomplished simply by employing a larger stainless jar (10-mL volume) and three 10-mm-diameter stainless ball with direct heating with a heat gun

(inner vessel temperature[23] (reaction temperature): 53 °C; preset temperature of heat gun: 80 °C). Under these conditions, 1.34 g (82%) of **2g** was obtained by ball milling after 30 min. Although 1-(phenanthrene-9-yl)pyrene (**1h**) and 1,1'-bipyrene (**1i**) were also transformable substrates and the reactions indeed proceeded, the cyclized product **2h** was isolated only in 25% yield, and we were not able to isolate **2i** using the usual isolation techniques under air. Similar to **2e** and **2f**, the low yield and decomposition of products are also rationalized by the instability of *bay*-region-reactive large PAHs.[22] Next, naphthalene-substituted PAHs **1j**, **1k**, **1l**, and **1m** were tested for anionic cyclodehydrogenation to examine the effects of five-, six-, and seven-membered ring containing molecules. Naphthylfluoranthene (**1j**), naphthlycorannulene (**1k**), and naphthylcoronene (**2l**) were less reactive even upon heating at 71 °C (heat-gun preset temperature: 140 °C), affording the products in low yields (**2j**: 20%; **2k**: 10%; **2l**: 7%) with the recovery of the starting compounds. Interestingly, the seven-membered ring-embedded substrate **1m** effectively reacted at 25 °C, and dibenzo[4,5:6,7]cyclohepta[1,2,3-*cd*]perylene (**2m**) was obtained in 75% yield. Once again, we performed a gram-scale reaction by heating at 71 °C (heat-gun preset temperature: 140 °C) for 50 min to obtain **2m** in an 86% yield (1.1 g). A two-fold cyclodehydrogenation of dinaphthylchrysene (**1n**) proceeded smoothly with heating at 71 °C, and tetrabenzo[*de,jk,qr,wx*]hexacene (**2n**) was obtained in high yield (95%). Compound **2n** is a new PAH with a molecular formula of $C_{38}H_{20}$ and core of tetra-*peri*-tetrabenzohexacene, so detailed analysis of its photophysical properties and density functional theory (DFT) calculations were also performed (see Supporting Information (SI) for details).

Next, we tested the reactions of isoquinoline- and quinoline-conjugated arene derivatives, which are also known as inert substrates for oxidative cyclodehydrogenation due to their electron-deficient properties.[15] While these reactions afforded aza-perylenes **2o**–**2s** in low to moderate yields (12–65%), the products were valuable because the nitrogen-embedded structures are otherwise difficult to synthesize by conventional organic synthesis. 5-Phenyldibenzo[*i,k*]phenanthridine, which our group synthesized in a previous study,[15c] was also transformed into aza-nanographene **2t**. Finally, we found that our mechanochemical anionic cyclodehydrogenation was also effective for the synthesis of triphenylene (**2u**) from *ortho*-terphenyl (**1t**), albeit with a moderate but inferior yield compared with the typical Scholl reaction with oxidants.[4] Taking into account the safety, efficiency, mass production potential, and applicability, the developed Li-mediated mechanochemical reaction possesses huge synthetic advantages over conventional solution-state reactions with potassium(0). Furthermore, our easy-to-operate reaction unveiled the first systematic investigation of the substrate scope and limitations of anionic cyclodehydrogenation.

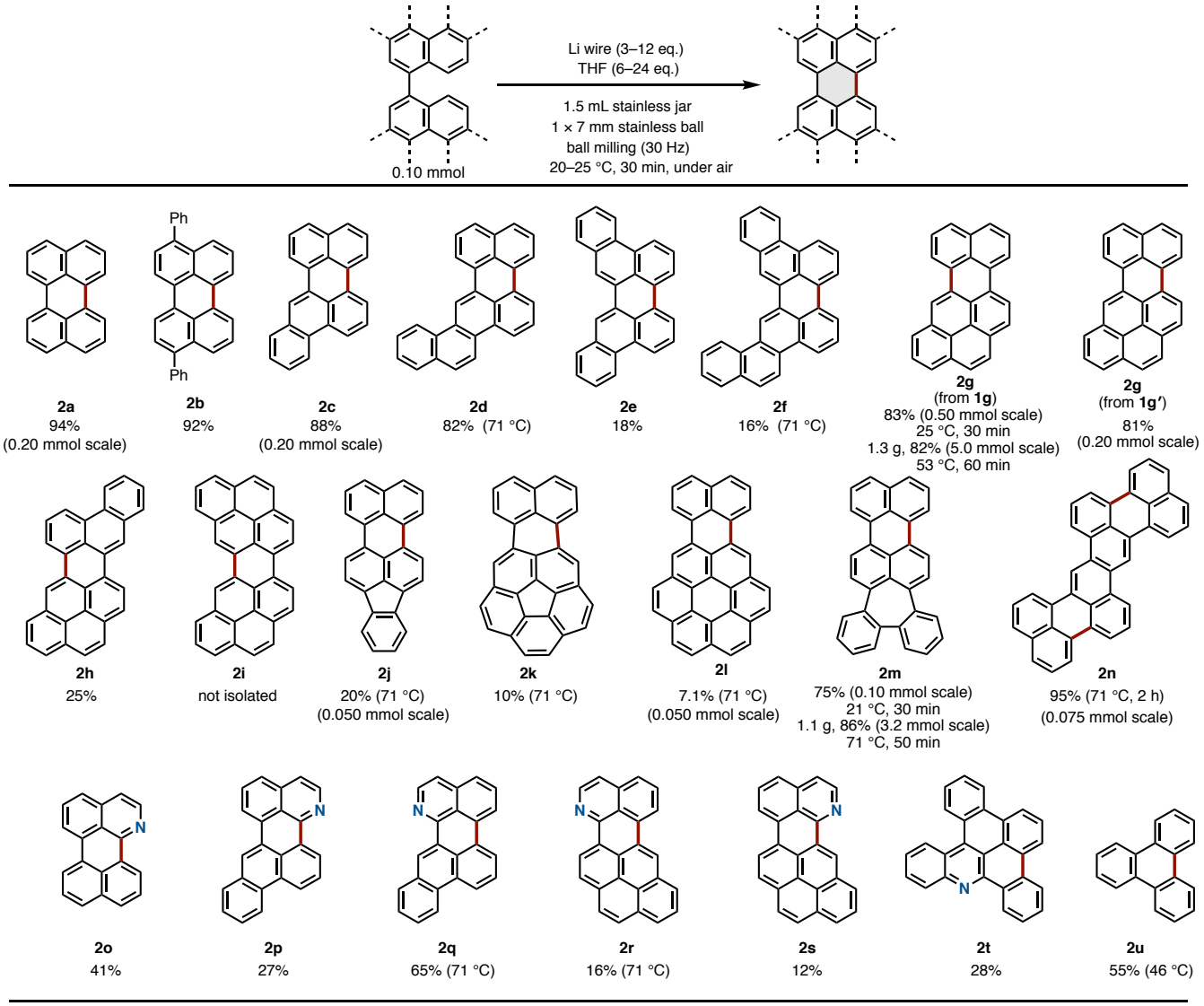

Figure 2. Substrate scope in lithium(0)-mediated mechanochemical anionic cyclodehydrogenation of binaphthyls and their analogues. Unless otherwise noted, 0.10 mmol of substrate (**1a**–**1u**) and a 7-mm diameter stainless-steel ball in a 1.5-mL stainless-steel jar were employed at room temperature (20–25 °C) for 30 min. For the gram-scale synthesis (3.2–5.0 mmol scale reaction) of **1g** and **1m**, three 10-mm diameter stainless-steel balls in a 10-mL stainless-steel jar were used. The reaction temperature/heat-gun preset temperature/reaction vessel volume: 34 °C/50 °C/1.5 mL; 46 °C/80 °C/1.5 mL; 53 °C/80 °C/10 mL; 71 °C/140 °C/1.5 mL; 71 °C/140 °C/10 mL. See Table S1 for details.

Mechanistic considerations by NMR spectroscopy

Next, we investigated the reaction mechanism, possible active species, and reaction profiles in the present solid-state lithium(0)-mediated anionic cyclodehydrogenation of 1,1′-binaphthyl (**1a**) based on the well-known mechanism of the potassium(0)-mediated solution-state reaction suggested by Scott.[13a] We also considered that **1a** first undergoes one-electron reduction by lithium(0) to form its radical anion $\mathbf{1a}^{\bullet-}$ which can receive an additional electron from lithium(0) to generate dianion $\mathbf{1a}^{2-}$ (Figure 3A). Dianion $\mathbf{1a}^{2-}$ can be transformed into the *trans*-dihydroperylene dianion $\mathbf{3a}^{2-}$. On the other hand, $\mathbf{1a}^{\bullet-}$ is also capable of cyclization to afford the *trans*-dihydroperylene radical anion $\mathbf{3a}^{\bullet-}$, which is also easily reduced by lithium(0) to give $\mathbf{3a}^{2-}$. As suggested in the potassium(0)-mediated reaction, equilibria between $\mathbf{1a}^{\bullet-}/\mathbf{3a}^{\bullet-}$ and $\mathbf{1a}^{2-}/\mathbf{3a}^{2-}$ likely exist in our lithium system. Finally, intermediate $\mathbf{3a}^{2-}$ would spontaneously and irreversibly provide perylene dianion $\mathbf{2a}^{2-}$ through the release of hydrogen gas.[13a] Based on this assumption, we attempted to directly observe the active species and/or intermediates by ^{1}H NMR spectroscopy. After the cyclodehydrogenation of **1a** under standard conditions at 25 °C for 30 min, a dark purple paste of the crude mixture was observed in the reaction vessel, which was directly analyzed by ^{1}H NMR after dilution with THF-d_8. Only perylene dianion $\mathbf{2a}^{2-}$, whose three hydrogen atom signals were largely shifted to a high magnetic field region up to 4.7 ppm (Figure 3B), was observed. In the ^{7}Li NMR analysis in THF-d_8, unreacted Li^0 (a broad peak between 0 and 4 ppm) and solvated $[Li^+(THF)_n]$ ion[24a] (a sharp peak at –0.98 ppm) were observed. There is no peak corresponding to strongly coordinated complexes such as $(Li^+)_2(\mathbf{2a}^{2-})$, whose ^{7}Li NMR peak should be observed in the higher magnetic region between –2 and –10 ppm.[24] The states of $\mathbf{2a}^{2-}$ and Li^+ in the solid-state are unknown at this stage, but the same type of state $(2[Li^+(THF)_n]$

+ [**2a**$^{2-}$(THF)$_n$) observed in the ^{1}H and ^{7}Li NMR spectra in THF-d_8 can be possible candidates because of the use of 6 eq. of THF most likely promoted the reaction in the solid state (Table 1, entry 1). While we could not observe other active species and were not able to measure solid-state NMRs, the observation of dianion **2a**$^{2-}$ as a species in the resting state supports the possible mechanism shown in Figure 3A. However, it should be emphasized that the current solid-state mechanochemical reaction is much faster than the solution-state long-time heating reaction with potassium(0), and all processes, including two one-electron reductions, cyclization, and dehydrogenation, quickly converge to the relatively stable perylene dianion, **2a**$^{2-}$. These phenomena are unprecedented in previous cyclodehydrogenations, and we believe that the higher reactivity of lithium has been showcased for the first time by utilizing the mechanochemical solid-state reaction.

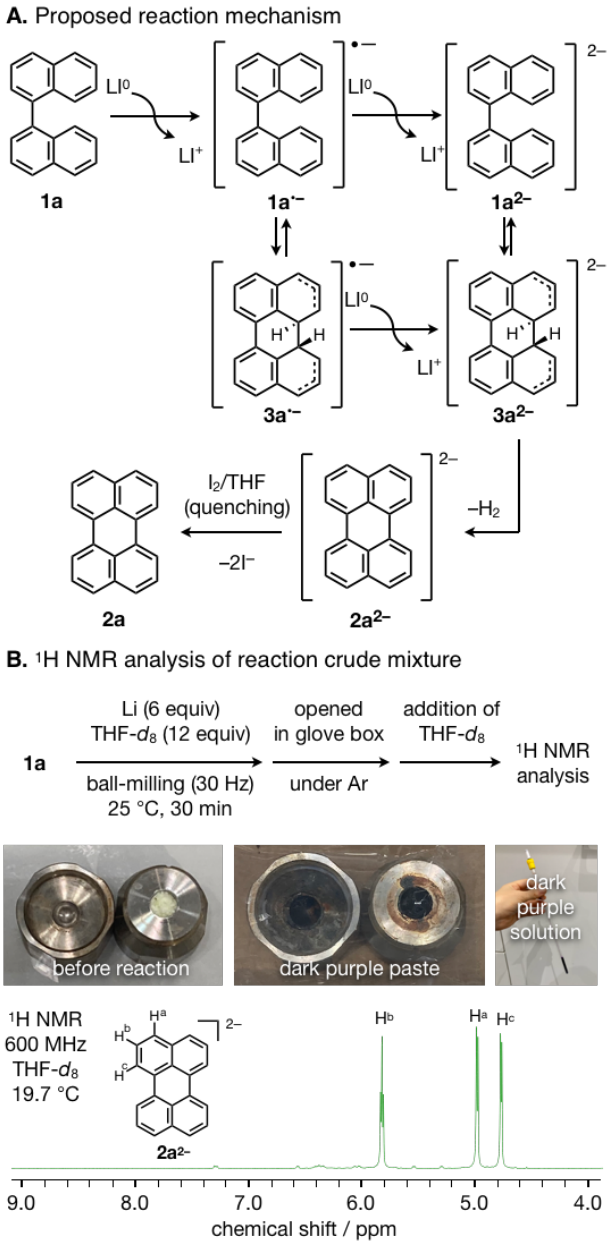

Figure 3. (**A**) Proposed reaction mechanism and (**B**) ^{1}H NMR analysis of crude mixture in the reaction of 1,1′-binaphthyl (**1a**) before quenching with I_2. The spectrum of a cold sample solution in THF-d_8 at −78 °C was measured at the room-temperature (19.7 °C).

One possible reason for such a rapid reaction is simply thought to be the efficient mechanical mixing of lithium(0) with the substrate to form a minute solid dispersion mixture, which efficiently promotes electron transfer from lithium(0) to the substrate. Of course, this can also occur when using other metals, such as sodium(0) and potassium(0), as we observed in the modification of the reaction conditions (Table 1, entries 12 and 13); however, these reactions did not proceed to completion within 30 min at 25 °C. This can also be rationalized by the highest reducing ability of lithium(0) among other metals (Figure 1A). More detailed and careful observations of the reactive species and morphological changes of the substate/additive/lithium(0) are needed for further investigation of the reaction mechanism.

Reaction profiles of anthracene-substituted biaryls

To understand the critical factor determining the reaction progress, we further tested the reactions of anthracene-substituted biaryls **1v**, **1w**, and **1w′** (Figure 4). In the reactions of **1v** and **1w**, the target cyclized products **2v** and **2w** were not obtained, and almost all starting materials remained unreacted. In contrast, the reaction of 1-(naphthalen-1-yl)anthracene (**1w′**) proceeded under slightly modified reaction conditions with lithium(0) or sodium(0) at 71 °C (heat-gun preset temperature: 140 °C) to afford benzoperylene **2w** in 10–21% yield. In these reactions, **1w′** was fully consumed; however, the product yields were consequently low because of the poor solubility and degradability of **2w**.

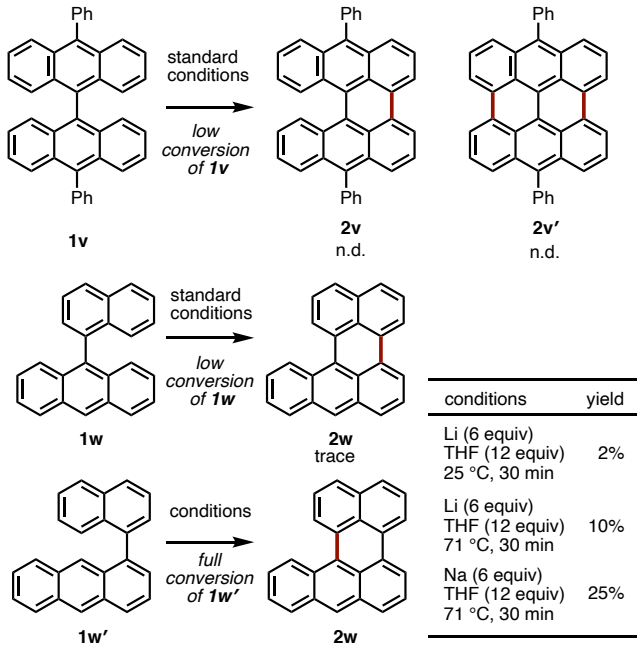

Figure 4. Reactions of anthracene-substituted biaryls. 0.20 mmol of substrates and a 7-mm diameter stainless-steel ball in a 1.5-mL stainless-steel jar were employed at 25–71 °C for 30 min.

Computational studies on activation energies in cyclization

Stimulated by the above-mentioned results in Figure 4 and the successful and unsuccessful cyclization of **1a**, **1j**, and **1m** in Figure 2, we performed computational considerations for the cyclization processes of each substrate (Figure 5). Related to a computational study, Puiatti and Jimenez recently reported the mechanistic investigations on anionic cyclodehydrogenation of 1,1′-binaphthyl (**1a**) by DFT.[13f] They revealed that the cyclization could preferentially occur from open-shell singlet dianion $\mathbf{1a}^{2-}$ ($\mathbf{1a}^{2-}$ (OS)) to $\mathbf{3a}^{2-}$ (OS) rather than radical anion $\mathbf{1a}^{\bullet-}$ to $\mathbf{3a}^{\bullet-}$, with an estimated activation barrier in the former of 26.1 kcal/mol by the symmetry-broken unrestricted B3LYP[25,26a,b] (SB-UB3LYP)/6-31+G(d)/IEF-PCM(toluene) level of theory at 363 K. We also examined the same type of calculations by the UB3LYP/6-31+G(d)/IEF-PCM(THF)[26c] level of theory at 298 K using a Gaussian 16 program.[27] For simplification of calculations, we calculated only radical anions and symmetry-broken open-shell singlet dianions, whereas closed-shell dianions and triplet dianions are excluded in this work due to those energetically unstable features as investigated by Puiatti and Jimenez.[13f] To evaluate the electron-accepting ability and stability of **1x**, $\mathbf{1x}^{\bullet-}$, $\mathbf{3x}^{\bullet-}$, $\mathbf{1x}^{2-}$ (OS), and $\mathbf{3x}^{2-}$ (OS) (**x** = **a**, **j**, **m**, **w**, **w′**), the relative free energy (ΔG, kcal/mol) of **1x** was estimated, taking into account the energies of free lithium(0) and Li^+ (Figure 5A). In these calculations, the absolute values of energy differences between **1x**/$\mathbf{1x}^{\bullet-}$/$\mathbf{1x}^{2-}$ and $\mathbf{3x}^{\bullet-}$/$\mathbf{3x}^{2-}$ are not useful because the presented one-electron reduction from atomic lithium(0) is not realistic, and there are many possibilities for the state of lithium(0) and Li^+ to be considered, such as lithium clusters, complexes with multiple anionic substrates, and THF molecules. However, it is easy to compare the relative stabilities and electron-accepting abilities of compounds in the same anionic state. For example, larger π-systems than **1a** clearly stabilize radical anions $\mathbf{1x}^{\bullet-}$ (**x** = **j**, **m**, **w**, **w′**) (ΔG = −16.0 ~ −22.8 kcal/mol vs. −8.8 kcal/mol) and dianions $\mathbf{1x}^{2-}$ (**x** = **j**, **m**, **w**, **w′**) (ΔG = −12.5 ~ −21.9 kcal/mol vs. +3.1 kcal/mol). In addition, based on the hypothesis that there is no equilibrium between **1x**/$\mathbf{1x}^{\bullet-}$/$\mathbf{1x}^{2-}$, we calculated the activation barriers ($\Delta G^{\ddagger}$) for each cyclization, that is, $\mathbf{TS_{1x\text{-}RA}}$ (radical anion pathway) and $\mathbf{TS_{1x\text{-}DA\text{-}OS}}$ (open-shell singlet dianion pathway) for the reactions of $\mathbf{1x}^{\bullet-}$ to $\mathbf{3x}^{\bullet-}$ and $\mathbf{1x}^{2-}$ (OS) to $\mathbf{3x}^{2-}$ (OS). Comparing the activation barriers of the radical anion and dianion pathways, the dianion pathways are favored for all substrates. To investigate the effects of the five- and seven-membered rings in the substrates, the activation barriers for the cyclization of $\mathbf{1j}^{2-}$ (OS) and that of $\mathbf{1m}^{2-}$ (OS) were compared. As a result, the activation barrier for the cyclization of **1m** via the dianion pathway is 2.4 kcal/mol lower than that for the cyclization of **1j**. Even via a radical anion, **1m** cyclization is favored by 3.8 kcal/mol. Indeed, the results are consistent with the experimental results that **2m** was obtained in high yield, whereas cyclization of **1j** did not occur at room temperature and required heating to achieve low yields (Figure 2). This can be rationalized by the higher electron-accepting ability of the five-membered aromatic ring in the fluoranthene core of $\mathbf{1j}^{2-}$. We believe that the higher stabilization of $\mathbf{1j}^{2-}$ compared to $\mathbf{1m}^{2-}$ can result in a relatively higher activation barrier. Indeed, the relative energy of $\mathbf{1j}^{2-}$ is largely stabilized by −21.9 kcal/mol upon two-electron reduction of **1j** by two Li(0), while the stabilization energy of $\mathbf{1m}^{2-}$ is estimated at −12.5 kcal/mol. Furthermore, a comparison of the activation barriers for the cyclization of **1w** and **1w′** shows that the activation barriers of **1w** are larger by 7.0 kcal/mol than those of **1w′**. Even via radical anions, **1w′** has a lower activation energy by 8.7 kcal/mol than that of **1w**. The calculated results are also consistent with the experimental results that **1w′** cyclizes easily, whereas **1w** does not undergo cyclization (Figure 4).

The differences in these reactivities arise from steric repulsion in the transition states, which are simply visualized by non-covalent interaction (NCI) plot analysis using the NCIPLOT4 program. (Figure 5B)[28] In this analysis, red-orange color-reduced density gradient isosurfaces correspond to the existence of repulsive interactions. Compared with the larger steric hindrance around the fjord-region in $\mathbf{TS_{1w\text{-}DA\text{-}OS}}$, the less hindered transition states, $\mathbf{TS_{1a\text{-}DA\text{-}OS}}$ and $\mathbf{TS_{1w'\text{-}DA\text{-}OS}}$, have lower activation barriers.

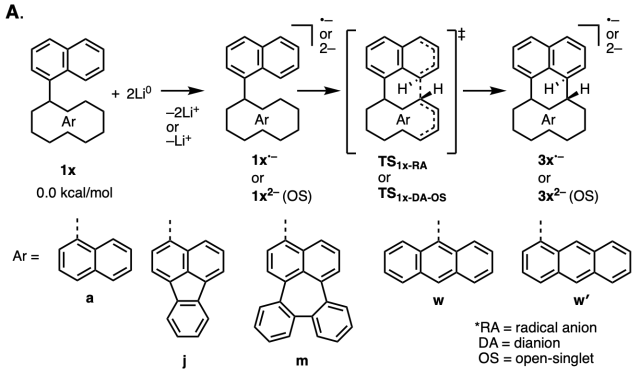

x	$\mathbf{1x}^{\bullet-}$	$\mathbf{TS_{1x\text{-}RA}}$	$\mathbf{3x}^{\bullet-}$	$\mathbf{1x}^{2-}$ (OS)	$\mathbf{TS_{1x\text{-}DA\text{-}OS}}$	$\mathbf{3x}^{2-}$ (OS)
a	−8.8	23.3 (32.1)	22.0	3.1	27.2 (24.1)	8.0
j	−22.8	13.4 (36.2)	6.0	−21.9	4.3 (26.2)	−11.8
m	−16.0	16.4 (32.4)	12.7	−12.5	11.4 (23.8)	−4.6
w	−19.5	22.4 (41.8)	20.5	−12.9	16.2 (29.1)	5.2
w′	−19.3	13.8 (33.1)	12.0	−13.9	8.1 (22.1)	−3.0

ΔG in kcal/mol calculated by UB3LYP/6-31+G(d) with IEF-PCM(THF) at 0 atm, 298.15 K. Activation energy ($\Delta G^{\ddagger}$) based on $\mathbf{1x}^{\bullet-}$ or $\mathbf{1x}^{2-}$ in parentheses.

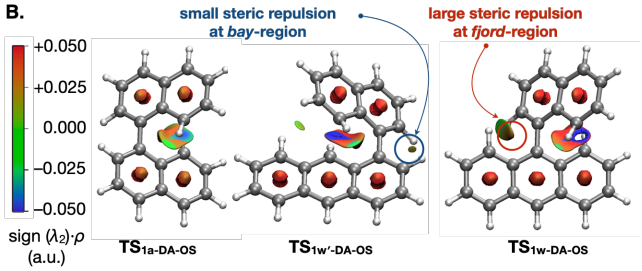

Figure 5. (**A**) Profile of free energies and activation energies in anionic cyclization estimated by DFT calculations. (**B**) NCI analysis[28] and reduced density gradient isosurfaces (isosurface value = 0.33) by a NCIPLOT4 program for $\mathbf{TS_{1a\text{-}DA\text{-}OS}}$, $\mathbf{TS_{1w\text{-}DA\text{-}OS}}$, and $\mathbf{TS_{1w'\text{-}DA\text{-}OS}}$. Color code based on sign (λ_2)ρ was −0.05 a.u. (blue) < 0.00 a.u. (green) < 0.05 a.u. (red). Blue and red isosurfaces show regions having attractive and repulsive interactions, respectively, and green isosurfaces show week van der Waals interactions such as π–π interaction.

Synthesis of novel nanographenes by multi-fold cyclodehydrogenation

Finally, we attempted multifold cyclodehydrogenation for the synthesis of unprecedented nanographenes as one of the highlighted applications of the present lithium(0)-mediated mechanochemical cyclodehydrogenation. First, C_3-symmetric benzo[*c*]naphtho[2,1-

p]chrysene (**4**), which is frequently considered a precursor for bucky bowls,[29b,c] was brominated to C_3-symmetric tribromide **4′** (Figure 6A).[29c] Suzuki–Miyaura coupling of **4′** with di-*tert*-butylnaphthalene pinacol boronate (**5**) afforded the precursor **6** in a 60% yield. Under anionic cyclodehydrogenation conditions with lithium(0) and heating at 71 °C (heat-gun preset temperature: 140 °C), a highly challenging three-fold cyclodehydrogenation proceeded to afford trifurcated perylene trimer **7** in a 38% yield. Compound **7** possesses a C_3-symmetric trifurcated structure with a central benzene junction and three perylene wings. The geometry optimization by DFT shows a slightly twisted structure, such as a propeller shape derived from three cove regions ([4]helicene moieties) (see SI). In the UV–vis absorption measurements of a solution of **7** in CH_2Cl_2 (c = 0.0461 mM), two absorption maxima in the long wavelength regions are observed at 478 and 451 nm, and shoulder absorption is extended up to 700 nm (Figure 6B).

In the depiction of frontier molecular orbitals calculated by B3LYP/6-31G(d), HOMO (–4.85 eV) and LUMO (–2.11 eV) are each degenerated, and molecular orbitals (MOs) are localized on two perylene wings (Figure 6C). On the other hand, HOMO–1 (–5.11 eV) is delocalized on an entire molecule. The observed absorptions are identical to the excitations simulated by time-dependent DFT (TD-DFT): HOMO to LUMO ($\lambda_{\text{TD-DFT}}$ = 502 nm, oscillation strength (f) = 0.5098) and HOMO(a) to LUMO+1 ($\lambda_{\text{TD-DFT}}$ = 453 nm, f = 0.4288) (see SI for details). Comparing the absorption spectra of **7** and **2n** (see SI), **7n** shows shorter wavelength absorptions and broader absorption peaks than **2n**. Moreover, the Stokes shift of **7** is larger than **2n**. These results indicate that **7** has a more flexible structure than **2n**, and the large structural relaxation in the excited state of **7** is considered to cause a larger Stokes shift than the rigid **2n**.

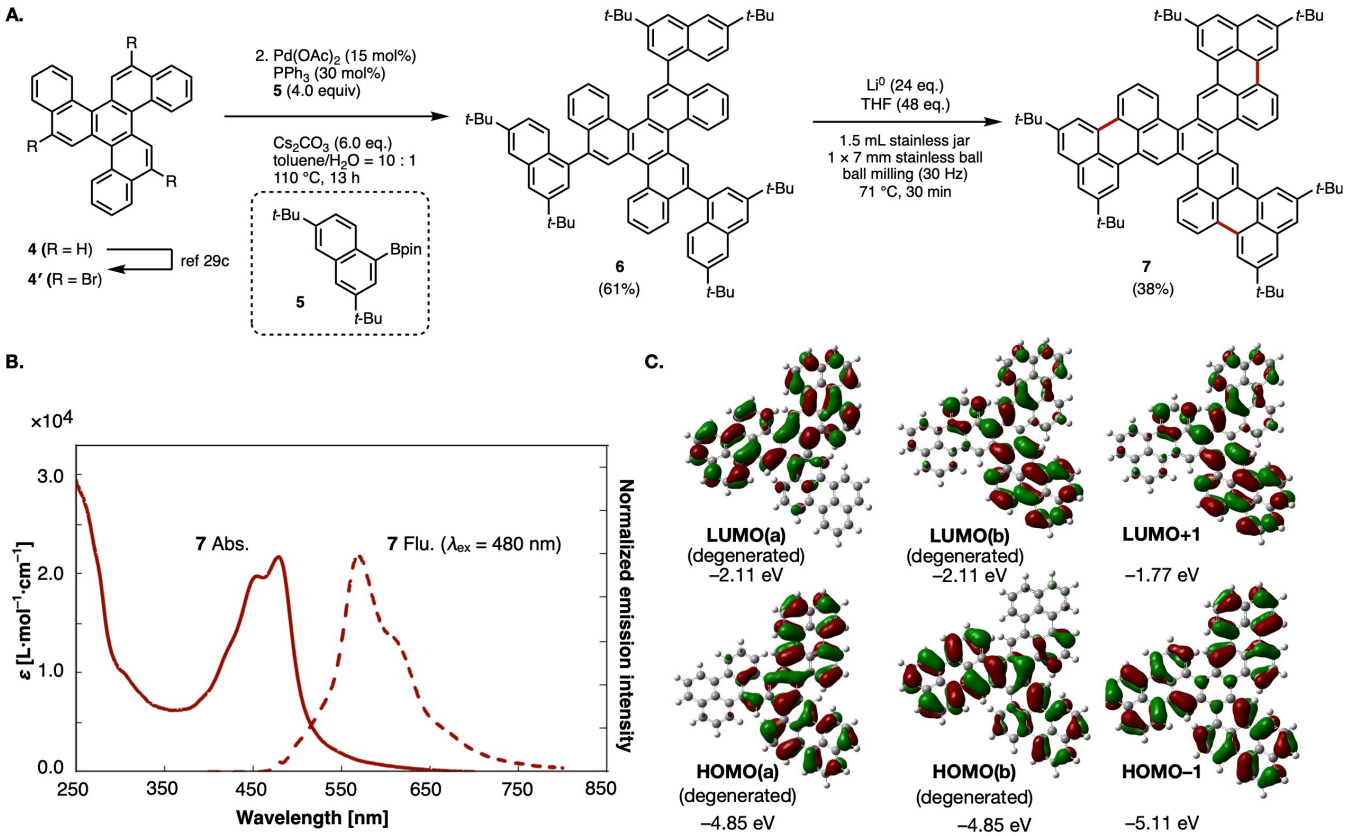

Figure 6. (**A**) Synthesis of C_3-symmetric perylene trimer **7**. (**B**) UV-Vis absorption and emission spectra of **7** (c = 0.0461 mM) in CH_2Cl_2. (**C**) Frontier molecular orbitals of **7**.

Finally, we tested the synthesis of non-substituted (pristine) quinterrylene (**9**)[30] from quinquenaphthalene (**8**) (Figure 7). Rylene or polyrylenes[31] are known as promising materials for organic electronic devices that show attractive photophysical, electrochemical, and magnetic properties,[32] and their polymeric structure is also now known as N = 5 armchair-type graphene nanoribbon[33] with a short width. Only pristine quaterrylene (four naphthalene units) was previously synthesized as the longest and analyzable non-substituted rylene, first by Clar and coworkers[34a] and later by Cataldo.[34b] They dimerized perylene to quaterrylene by a typical Scholl reaction using $AlCl_3$ or a mixture of $FeCl_3$ and $AlCl_3$. Moreover, Johnson and coworkers recently found that quaterrylene could be synthesized in high yield by the dimerization reaction of perylene with DDQ and TfOH in refluxing dichloromethane for 24 h.[34c] The generated crude quaterrylene was purified by repeated washing with THF because of its insolubility. We anticipated that our lithium-mediated solid-state reaction would be adequate for the reaction and synthesis of poorly soluble compounds such as quinterrylene **9** without the need for solubilizing substituents and reaction termination induced by the exclusion of insoluble intermediates from the reaction media.

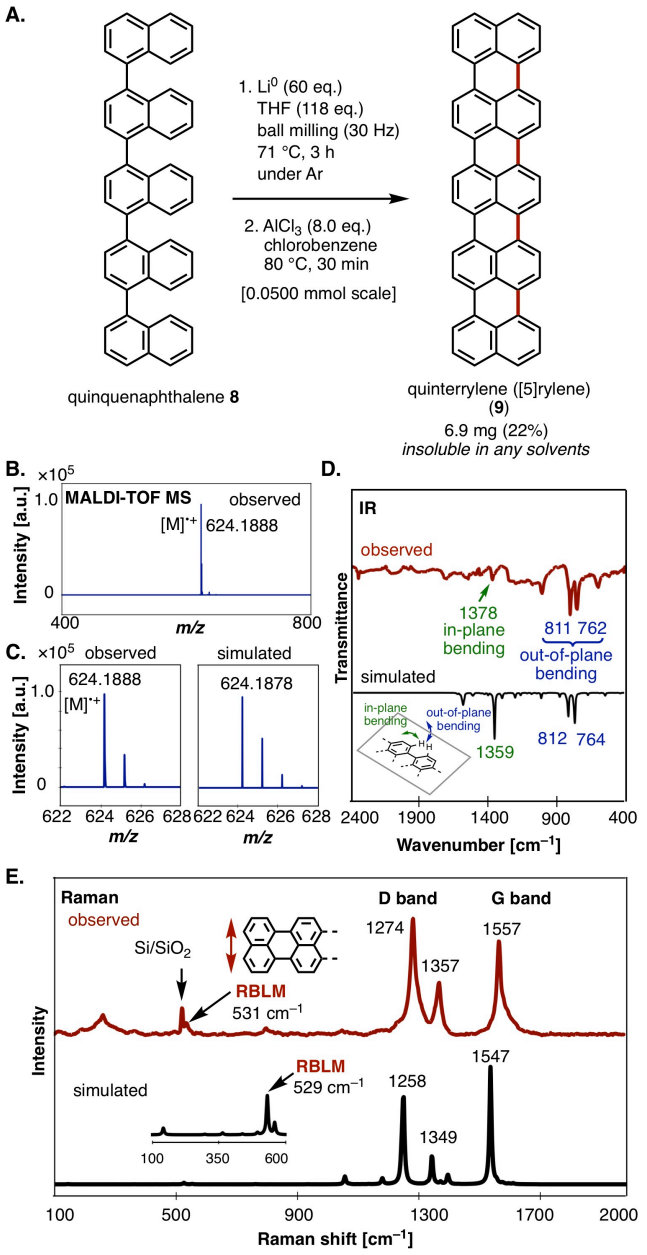

Figure 7. (**A**) Cyclodehydrogenation of quinquenaphthalene **8** to pristine quinterrylene **9**. (**B**) MALDI-TOF MS spectrum of **9**. (**C**) Observed (left) and simulated (right) isotopic patterns of **9** in MALDI-TOF MS. (**D**) Observed IR spectrum of **9** and a simulated IR spectrum by DFT/PBE0/def2-SVP. (**E**) Observed Raman spectrum of **9** on silicon surface with a 632 nm laser and a simulated Raman spectrum by DFT/PBE0/def2-SVP. Simulated IR and Raman spectra are scaled with a scaling factor of 0.95427.[35]

Thus, we attempted to transform readily prepared quinquenaphthalene **8** into **9** (Figure 7A). Initial investigations revealed that treating **8** with excess Li and THF resulted in the formation of black insoluble materials with $m/z = 624$, which correlates to the mass of **9**. However, there were some inseparable mass peaks, such as $m/z = 626$, 628, and 640, which are considered to be the peaks of partially cyclized products and/or by-products with an oxygen atom. After modifying the reaction conditions, we found that the reaction of **8** with 60 eq. of Li and 118 eq. of THF with heating at 71 °C (heat-gun preset temperature: 140 °C) for 3 h under a rough argon atmosphere, followed by treatment of the crude mixture with $AlCl_3$ in chlorobenzene[32f] at 80 °C for 30 min, afforded a relatively simple crude mixture, which was purified by washing with hot toluene with a Soxhlet extraction apparatus.

The resulting black powder was analyzed using matrix-assisted laser desorption/ionization time-of-flight mass spectrometry (MALDI-TOF MS) to obtain an intense mass peak at $m/z = 624.1888$ (Figure 7B), with m/z values and isotopic patterns identical to those of $[\mathbf{9}]^{+}$ (Figure 7C). To further elucidate the structure of the product, we measured the IR and Raman spectra (Figures 7D and 7E). In the IR spectrum, there were some characteristic peaks in the fingerprint region, such as 762 and 811 cm^{-1}. These correspond to the vibrations of the out-of-plane bending mode in the *bay*-region C–H bonds, which were well reproduced by DFT calculations (see SI). The observed peak at 1378 cm^{-1} was weak but identical to that of the in-plane bending mode. Generally, the Raman spectra of graphene and graphene nanoribbons provide important information about the structure, defects, width, aspect ratio, and defects. In previous similar measurements of $N = 5$ armchair-type graphene nanoribbon,[33] a radial breathing-like vibration mode (RBLM(observed)[33a–c]: 532 cm^{-1}; RBLM(simulated)[33f,g]: 521–545 cm^{-1}), D band (1300–1350 cm^{-1}), and G band (1564–1580 cm^{-1}) have been reported to elucidate the rylene structure. In our measurement (red line in Figure 7E), RBLM mode, G band, and D band were observed at 531, 1274, and 1557 cm^{-1}, respectively. These values are very similar to the reported values and the values simulated by the DFT/B3LYP/def2-SVP level of theory (black line in Figure 7E). Based on the direct evidence of the MALDI-TOF MS spectrum as well as indirect evidence in IR and Raman measurements, it is reasonable to state that we successfully synthesized quinterrylene **9**.

Conclusions

In this study, we have developed a mechanochemical anionic cyclodehydrogenation reaction using lithium(0). First, we investigated various conditions for the cyclization of binaphthyl to perylene and found that the cyclodehydrogenation proceeded by ball milling with easy-to-handle lithium(0)-wire and a small amount of THF as an additive at room temperature under air for 5 min. Compared with solution-state reactions with potassium(0) and lithium(0) and solid-state reactions with sodium(0) and potassium(0), the present method shows significant synthetic benefits in terms of handleability under air, rapid reactivity at room temperature, safety, and practical gram-scale synthesis. With this simple and easy synthetic tool in hand, we investigated a wide range of substrate scopes and synthesized various novel polycyclic aromatic compounds for the first time. ^{1}H NMR spectroscopic analysis of the dark purple crude paste of the reaction mixture clearly showed the formation of a perylene dianion, which is a similar resting intermediate in the solution-state reaction. While the mechanism of the present solid-state reaction can be different from the mechanism proposed for the solution-state reaction, we expect that efficient mechanochemical mixing in the solid state could bring out the potent highest reactivity (reducing ability) of lithium(0), resulting in rapid cyclodehydrogenation. Furthermore, we were able to synthesize and characterize novel polycyclic aromatic compounds such as **2n** and **7** via multifold cyclodehydrogenation. In particular, we synthesized quinterrylene **9**, the longest known non-substituted pristine rylene, which is difficult to

synthesize due to its low solubility. MALDI-TOF MS, IR, and Raman spectroscopic analyses support the formation of **9**.

The mechanochemical anionic cyclodehydrogenation with lithium described in this study is an innovative and practical method for the rapid and efficient synthesis of polycyclic compounds. This protocol not only allows the cyclization of polyarylenes that do not proceed in the solution state but is also applicable to the synthesis of insoluble compounds. We hope that this reaction can be used universally in the future, leading to the development of a variety of unexplored polycyclic aromatic compounds and molecular nanocarbons.

ASSOCIATED CONTENT

Supporting Information

Supporting Information is available free of charge on the publication website. Experimental procedures, ^{1}H, ^{13}C and ^{7}Li NMR spectra, characterization of data for all new compounds, optical properties, and computational data.

AUTHOR INFORMATION

Corresponding Author

* ito.hideto.p4@f.mail.nagoya-u.ac.jp (H.I.)
* itami@chem.nagoya-u.ac.jp (K.I.)

ACKNOWLEDGMENT

This study was supported by the JST-CREST program (JPMJCR19R1 to H.I.), JSPS KAKENHI (Grant No. JP19H05463 to K.I., JP21H01931 to H.I.), and Foundation of Public Interest of Tatematsu (to H.I.). H.I. would like to thank the Verder-Scientific Award (IRMAIL Science Grand 2017) for launching and funding the project of mechanochemical synthesis of nanocarbons. We thank Dr. Satoshi Kurumada (Nagoya University) for a fruitful discussion on this work. DART MS measurements were conducted using resources from the Chemical Instrumentation Facility (CIF), Research Center for Materials Science (RCMS), Nagoya University. The computations were performed using the Research Center for Computational Science, Okazaki, Japan (Project Nos.:21-IMS-C070 and 22-IMS-C069), and the SuperComputer System, Institute for Chemical Research, Kyoto University. ITbM was supported by the World Premier International Research Center Initiative (WPI), Japan. The authors declare no competing financial interests.

REFERENCES

(1) (a) Guo, Y.; Li, H.; Zhai, T. Reviving Lithium-Metal Anodes for Next-Generation High-Energy Batteries. *Adv. Mater.* **2017**, *29*, 1700007. (b) Tarascon, J.-M.: Armand, M. Issues and challenges facing rechargeable lithium batteries. *Nature* **2001**, *414*, 359. (c) Goodenough, J. B.; Park, K.-S. The Li-Ion Rechargeable Battery: A Perspective. *J. Am. Chem. Soc.* **2013**, *135*, 1167. (d) Yoshino, A.; Sanechika, K.; Nakajima, T. Secondary battery. Patent JP1989293, May 15, 1985.

(2) (a) Birch, A. J. 117. Reduction by dissolving metals. Part I. *J. Chem. Soc.* **1944**, 430. (b) Wilds, A. L.; Nelson, N. A. A Superior Method for Reducing Phenol Ethers to Dihydro Derivatives and Unsaturated Ketones. *J. Am. Chem. Soc.* **1953**, *75*, 5360. (c) Hook, J. M.; Mander. L. N. Recent developments in the Birch reduction of aromatic compounds: applications to the synthesis of natural products. *Nat. Prod. Rep.* **1986**, *3*, 35. (d) Zimmerman, H. E. A Mechanistic Analysis of the Birch Reduction. *Acc. Chem. Res.* **2012**, *45*, 164.

(3) Atomization enthalpy: (a) James, A. M.; Lord, M. P. in *Macmillan's Chemical and Physical Data*, Macmillan, London, UK, 1992. ISBN: 978-0333511671. (b) Other data of atomization enthalpy: 159.4 kJ/mol (for Li), 107.3 kJ/mol (for N), 89.2 kJ/mol (for K). Ellis, H. (Ed.) in *Nuffield Advanced Science: Book of Data*, Revised Edition, Longman, London, UK, 1984. ISBN: 9780582354487.

(4) Reviews on Scholl reaction: (a) Grzybowski, M.; Skonieczny, K.; Butenschön, H.; Gryko, D. T. Comparison of Oxidative Aromatic Coupling and the Scholl Reaction. *Angew. Chem., Int. Ed.* **2013**, *52*, 9900. (b) Grzybowski, M.; Skonieczny, K.; Butenschön, Gryko, D. T. Synthetic Applications of Oxidative Aromatic Coupling—From Biphenols to Nanographenes. *Angew. Chem., Int. Ed.* **2020**, *59*, 2998. (c) Jassasa, R. S.; Mughal, E. U.; Sadiqc, A.; Alsantalid, R. I.; Al-Rooqie, M. M.; Naeem, N.; Moussa, Z.; Ahmed, S. A. Scholl reaction as a powerful tool for the synthesis of nanographenes: a systematic review. *RSC Adv.* **2021**, *11*, 32158. (d) Zhan, Y.; Pun, S. H.; Miao, Q. The Scholl Reaction as a Powerful Tool for Synthesis of Curved Polycyclic Aromatics. *Chem. Rev.* **2022**, *122*, 14554

(5) Early examples of Scholl reaction: (a) Scholl, R.; Mansfeld, J. *Ber. Dtsch. Chem. Ges.* **1910**, *43*, 1734. (b) Homer, A. J. *Chem. Soc. Trans.* **1910**, *97*, 1141.

(6) PAHs and molecular nanocarbons: (a) Segawa, Y.; Ito, H.; Itami, K. Structurally uniform and atomically precise carbon nanostructures. *Nat. Rev. Mater.* **2016**, *1*, 15002. (b) Segawa, Y.; Levine, D. R.; Itami, K. Topologically Unique Molecular Nanocarbons. *Acc. Chem. Res.* **2019**, *52*, 2760. (c) Panwar, N.; Soehartono, A. M.; Chan, K. K.; Zeng, S.; Xu, G.; Qu, J.; Coquet, P.; Yong, K-T.; Chen, X. Nanocarbons for Biology and Medicine: Sensing, Imaging, and Drug Delivery. *Chem. Rev.* **2019**, *119*, 9559. (d) Tielens, A. G. G. M. Interstellar Polycyclic Aromatic Hydrocarbon Molecules. *Annu. Rev. Astron. Astrophys.* **2008**, 46, 289. (e) Harvey, R. G. Polycyclic Aromatic Hydrocarbons, Wiley-VCH, New York, 1997.

(7) Selected reviews on molecular nanocarbon synthesis: (a) Wu, J.; Pisula, W.; Müllen, K. Graphenes as Potential Material for Electronics. *Chem. Rev.* **2007,** *107*, 718. (b) Sun, Z.; Ye, Q.; Chi, C.; Wu, J. Low band gap polycyclic hydrocarbons: from closed-shell near infrared dyes and semiconductors to open-shell radicals. *Chem. Soc. Rev.* **2012**, *41*, 7857. (c) Stępień, M.; Gońka, E.; Żyła, M.; Sprutta, N. Heterocyclic Nanographenes and Other Polycyclic Heteroaromatic Compounds: Synthetic Routes, Properties, and Applications. *Chem. Rev.* **2017**, *117*, 3479. (d) Borissov, A.; Maurya, Y. K.; Moshniaha, L.; Wong, A.-S.; Żyła-Karwowska, M.; Stępień, M. Recent Advances in Heterocyclic Nanographenes and Other Polycyclic Heteroaromatic Compounds. *Chem. Rev.* **2022**, *122*, 565. (e) Stepek, I. A. Nagase, M.; Yagi, A.; Itami, K. New paradigms in molecular nanocarbon science. *Tetrahedron* **2022**, *123*, 132907.

(8) Selected examples and reviews of warped nanographenes synthesized by cyclodehydrogenation: (a) Kawasumi, K.; Zhang, Q.; Segawa, Y.; Scott, L. T.; Itami, K. A grossly warped nanographene and the consequences of multiple odd-membered-ring defects. *Nat. Chem.* **2013**, *5*, 739. (b) Feng, C.-N.; Kuo, M.-Y.; Wu, Y.-T. Synthesis, Structural Analysis, and Properties of [8]Circulenes. *Angew. Chem., Int. Ed.* **2013**, *52* 7791. (c) Sakamoto, Y.; Suzuki, T. Tetrabenzo[8]Circulene: Aromatic Saddles from Negatively Curved Graphene. *J. Am. Chem. Soc.* **2013**, *135*, 14074. (d) Cheung, K. Y.; Xu, X.; Miao, Q. Aromatic Saddles Containing Two Heptagons. *J. Am. Chem. Soc.* **2015**, *137*, 3910. (e) Cheung, K. Y.; Chan, C. K.; Liu, Z.; Miao, Q. A Twisted Nanographene Consisting of 96 Carbon Atoms. *Angew. Chem., Int. Ed.* **2017**, *56*, 9003. (f) Pun, S. H.; Miao, Q. Toward Negatively Curved Carbons. *Acc. Chem. Res.* **2018**, *51*, 1630. (g) Xia, Z.; Pun, S. H.; Chen, H.; Miao, Q. Synthesis of Zigzag Carbon Nanobelts through Scholl Reactions. *Angew. Chem., Int. Ed.* **2021**, 60, 10311. (h) Chaolumen, Stepek, I. A.; Yamada, K. E.; Ito, H.; Itami, K. Construction of Heptagon-

Containing Molecular Nanocarbons. *Angew. Chem., Int. Ed.* **2021**, *60*, 23508. (i) Konishi, A.; Yasuda, M. Breathing New Life into Nonalternant Hydrocarbon Chemistry: Syntheses and Properties of Polycyclic Hydrocarbons Containing Azulene, Pentalene, and Heptalene Frameworks. *Chem. Lett.* **2021**, *50*, 195. (j) Miera, G. G.; Matsubara, S.; Kono, H.; Murakami, K.; Itami, K. Synthesis of octagon-containing molecular nanocarbons. *Chem. Sci.* **2022**, *13*, 1848.

(9) Chemical synthetic reviews on graphene nanoribbon: (a) Narita, A.; Wang, X. Y.; Feng, X.; Müllen, K. New advances in nanographene chemistry. *Chem. Soc. Rev.* **2015**, *44*, 6616. (b) Yoon, K.-Y.; Dong, G. Liquid-phase bottom-up synthesis of graphene nanoribbons. *Mater. Chem. Front.* **2020**, *4*, 29.

(10) Ponugoti, N.; Parthasarathy, V. Rearrangements in Scholl Reaction. *Chem. Eur. J.* **2022**, *28*, e202103530.

(11) Aromatic rearrangements in Scholl reaction of 1,1′-binaphthyl and related aromatics: (a) Kovacic, P.; Koch, F. W. Coupling of Naphthalene Nuclei by Lewis Acid Catalyst—Oxidant. *J. Org. Chem.* **1965**, *30*, 3176. (b) Krishnamurti, R.; Kuivila, H. G.; Shaik, N. S.; Zubieta, J. Synthesis and Chemistry of Novel 2,2'-Binaphthyl-substituted Organotin Lewis Acids. *Organometallics* **1991**, *10*, 423. (c) Skraba-Joiner, S. L.; Mclaughlin, E. C.; Ajaz, A.; Thamatam, R.; Johnson, R. P. Scholl Cyclizations of Aryl Naphthalenes: Rearrangement Precedes Cyclization. *J. Org. Chem.* **2015**, *80*, 9578. (d) Han, Y.; Li, G.; Gu, Y.; Ni, Y.; Dong, S.; Chi, C. Formation of Azulene-Embedded Nanographene: Naphthalene to Azulene Rearrangement During the Scholl Reaction. *Angew. Chem., Int. Ed.* **2020**, *132*, 9111.

(12) Unsuccessful examples in Scholl reaction of electron-deficient arylenes: (a) Gryko, D. T.; Piechowska, J.; Gałezowski, M. Strongly Emitting Fluorophores Based on 1-Azaperylene Scaffold *J. Org. Chem.* **2010**, *75*, 1297. (b) Graczyk, A.; Murphy, F. A.; Nolan, D.; Fernández-Moreira, V.; Lundin, N. J.; Fitchett, C. M.; Draper, S. M. Terpyridine-fused polyaromatic hydrocarbons generated via cyclodehydrogenation and used as ligands in Ru(II) complexes. *Dalton Trans.* **2012**, *41*, 7746. (c) Sadhukhan, S. K.; Viala, C.; Gourdon, A. Syntheses of Hexabenzocoronene Derivatives. *Synthesis* **2003**, *10*, 1521. Also see ref 15c and 15e.

(13) Potassium(0)-mediated anionic cyclodehydrogenation of 1,1′-binaphthyl and its analogues in the solution state: (a) Rickhaus, M.; Belanger, A. P.; Wegner, H. A.; Scott, L. T. An Oxidation Induced by Potassium Metal. Studies on the Anionic Cyclodehydrogenation of 1,1′-Binaphthyl to Perylene *J. Org. Chem.* **2010**, *75*, 7358. (b) Kawasumi, K.; Mochida, K.; Kajino, T.; Segawa, Y.; Itami, K. $Pd(OAc)_2$/*o*-Chloranil/$M(OTf)_n$: A Catalyst for the Direct C–H Arylation of Polycyclic Aromatic Hydrocarbons with Boryl-, Silyl-, and Unfunctionalized Arenes. *Org. Lett.* **2012**, *14*, 418. (c) Markiewicz, J. T.; Wudl, F. Perylene, Oligorylenes, and Aza-Analogs. *ACS Appl. Mater. Interfaces* **2015**, *7*, 28063. (d) Eaton, S. W.; Miller, A. A.; Margulies, E. A.; Shoer, L. E.; Schaller, R. D.; Wasielewski, M. R. Singlet Exciton Fission in Thin Films of *tert*-Butyl-Substituted Terrylenes. *J. Phys. Chem. A* **2015**, *119*, 4151. (e) Uchida, Y.; Hirose, T.; Nakashima, T.; Kawai, T.; Matsuda, K. Synthesis and Photophysical Properties of a 13,13′-Bibenzo[*b*]perylenyl Derivative as a π-Extended 1,1′-Binaphthyl Analog. *Org. Lett.* **2016**, *18*, 2118. (f) Borioni, J. L.; Baumgartner, M. T.; Puiatti, M.; Jimenez, L. B. 1-Substituted Perylene Derivatives by Anionic Cyclodehydrogenation: Analysis of the Reaction Mechanism. *ACS Omega* **2022**, *7*, 21860. (g) Zhou, Z.; Egger, D. T.; Hu, C.; Pennachio, M.; Wei, Z.; Kawade, R. K.; Üngör, Ö.; Gershoni-Poranne, R.; Petrukhina, M. A.; Alabugin, I. V. Localized Antiaromaticity Hotspot Drives Reductive Dehydrogenative Cyclizations in Bis- and Mono-Helicenes. *J. Am. Chem. Soc.* **2022**, *144*, 12321.

(14) Early examples of anionic cyclodehydrogenation and related observations: (a) Solodovnikov, S. P.; Zaks, Y. B.; Ioffe, S. T.; Kabachnik, M. I. Radiospektrosk. Kvantovokhim. *Metody Strukt. Issled.* **1967**, 106; *Chem. Abstr.* accession no. 1969:28235; CAN 70:28235. (b) Solodovnikov, S. P.; Ioffe, S. T.; Zaks, Y. B.; Kabachnik, M. I. *Izv. Akad. Nauk SSSR, Ser. Khim.* **1968**, 442; *Chem. Abstr.* accession no. 1968:476168; CAN 69:76168; English translation: *Bull. Acad. Sci. USSR, Div. Chem. Sci.* **1968**, 442. (c) Ayalon, A.; Rabinovitz, M. Reductive ring closure of helicenes. *Tetrahedron Lett.* **1992**, *33*, 2395.

(15) Synthesis of electron-deficient polycyclic heteroaromatics by potassium(0)-mediated cyclodehydrogenation: (a) Firmansyah, D.; Banasiewicz, M.; Deperasińska, I.; Makarewicz, A.; Kozankiewicz, B.; Gryko, D. T. Vertically π-Expanded Imidazo[1,2-*a*]pyridine: The Missing Link of the Puzzle. *Chem. Asian J.* **2014**, *9*, 2483. (b) Firmansyah, D.; Banasiewicz, M.; Gryko, D. T. Vertically-expanded imidazo[1,2-*a*]pyridines and imidazo[1,5-*a*]pyridine via dehydrogenative coupling. *Org. Biomol. Chem.* **2015**, *13*, 1367. (c) Kawahara, K. P.; Matsuoka, W.; Ito, H.; Itami, K. Synthesis of Nitrogen-Containing Polyaromatics by Aza-Annulative π-Extension of Unfunctionalized Aromatics. *Angew. Chem., Int. Ed.* **2020**, *59*, 6383. (d) Zhang, P.-F.; Zeng, J.-C.; Zhuang, F.-D.; Zhao, K.-X.; Sun, Z.-H.; Yao, Z.-F.; Lu, Y.; Wang, X.-Y.; Wang, J.-Y.; Pei. J. Parent B_2N_2-Perylenes with Different BN Orientations. *Angew. Chem., Int. Ed.* **2021**, *60*, 23313. (e) Wang, C.-S.; Sun, Q.; García, F.; Wang, C.; Yoshikai, N. Robust Cobalt Catalyst for Nitrile/Alkyne [2+2+2] Cycloaddition: Synthesis of Polyarylpyridines and Their Mechanochemical Cyclodehydrogenation to Nitrogen-Containing Polyaromatics. *Angew. Chem., Int. Ed.* **2021**, *60*, 9627.

(16) Reviews on nanographene synthesis by our group: (a) Itami K. Toward controlled synthesis of carbon nanotubes and graphenes. *Pure Appl. Chem.* **2012**, *84*, 907. (b) Ito, H.; Ozaki, K.; Itami, K. Annulative π-Extension (APEX): Rapid Access to Fused Arenes, Heteroarenes, and Nanographenes. *Angew. Chem., Int. Ed.* **2017**, *56*, 11144. (c) Ito, H.; Segawa, Y.; Murakami, K.; Itami K. Polycyclic Arene Synthesis by Annulative π-Extension. *J. Am. Chem. Soc.* **2019**, *141*, 3. Also see ref 6a, 6b, 8h and 8j.

(17) Our previous contributions toward the development of novel synthetic methodology for PAHs and nanographenes: (a) Mochida, K.; Kawasumi, K.; Segawa, Y.; Itami. K. Direct Arylation of Polycyclic Aromatic Hydrocarbons through Palladium Catalysis. *J. Am. Chem. Soc.* **2011**, *133*, 10716. (b) Ozaki, K.; Kawasumi, K.; Shibata, M.; Ito, H.; Itami, K. One-shot K-region-selective annulative π-extension for nanographene synthesis and functionalization. *Nat. Commun.* **2015**, *6*, 6251. (c) Matsuoka, W.; Ito, H.; Itami, K. Rapid Access to Nanographenes and Fused Heteroaromatics by Palladium-Catalyzed Annulative π-Extension Reaction of Unfunctionalized Aromatics with Diiodobiaryls. *Angew. Chem., Int. Ed.* **2017**, *56*. 12224. (d) Koga, Y.; Kaneda, T.; Saito, Y.; Murakami, K.; Itami, K. Synthesis of partially and fully fused polyaromatics by annulative chlorophenylene dimerization. *Science* **2018**, *359*, 435. (e) Matsubara, S.; Koga, Y.; Segawa, Y.; Murakami, K.; Itami, K. Creation of negatively curved polyaromatics enabled by annulative coupling that forms an eight-membered ring. *Nat. Catal.* **2020**, *3*, 710. (f) Matsuoka, W.; Ito, H.; Sarlah, D.; Itami, K. Diversity-oriented synthesis of nanographenes enabled by dearomative annulative π-extension. *Nat. Commun.* **2021**, *12*, 3940. (g) Krzeszewski, M.; Ito, H.; Itami, H. Infinitene: A Helically Twisted Figure-Eight [12]Circulene Topoisomer. *J. Am. Chem. Soc.* **2022**, *144*, 862. (h) Matsuoka, W.; Kawahara, K. P.; Ito, H.; Sarlah, D.; Itami, K. π-Extended Rubrenes via Dearomative Annulative π-Extension Reaction. *J. Am. Chem. Soc.* **2023**, *145*, 658. (i) Kawahara, K. P.; Ito, H.; Itami, K. Rapid access to polycyclic thiopyrylium compounds from unfunctionalized aromatics by thia-APEX reaction. *Chem. Commun.* **2023**, Advanced Article. DOI: 10.1039/D2CC06706D. Also see Ref. 8a and 15c.

(18) Wang, G.-W.; Komatsu, K.; Murata, Y.; Shiro, M. Synthesis and X-ray structure of dumb-bell-shaped C_{120}. *Nature* **1997**, *387*, 583.

(19) Selected reviews on mechanochemical synthesis: (a) James, S. L.; Adams, C. J.; Bolm, C.; Braga, D.; Collier, P.; Friščić, T.; Grepioni, F.; Harris, K. D. M.; Hyett, G.; Jones, W.; Krebs, A.; Mack, J.; Maini, L.; Orpen, A. G.; Parkin, I. P.; Shearouse, W. C.; Steed, J. W.; Waddell, D. C. Mechanochemistry: opportunities for new and

cleaner synthesis. *Chem. Soc. Rev.* **2012**, *41*, 413. (b) Wang, G.-W. Mechanochemical organic synthesis. *Chem. Soc. Rev.* **2013**, *42*, 7668. (c) Do, J.-L.; Friščić, T. Mechanochemistry: A force of Synthesis. *ACS Cent. Sci.* **2017**, *3*, 13. (d) Hernández, J. G.; Bolm, C. Altering Product Selectivity by Mechanochemistry. *J. Org. Chem.* **2017**, *82*, 4007. (e) Howard, J. L.; Cao, Q.; Browne, D. L. Mechanochemistry as an emerging tool for molecular synthesis: what can it offer? *Chem. Sci.* **2018**, *9*, 3080. (f) Andersen, J.; Mack, J. Mechanochemistry and organic synthesis: from mystical to practical. *Green Chem.* **2018**, *20*, 1435. (g) Tan, D.; Friščić, T. Mechanochemistry for Organic Chemists: An update. *Eur. J. Org. Chem.* **2018**, 18. (h) Tan, D.; García, F. Main group mechanochemistry: from curiosity to established protocols. *Chem. Soc. Rev.* **2019**, *48*, 2274. (i) Bolm, C.; Hernández, J. G. Mechanochemistry of Gaseous Reactants. *Angew. Chem., Int. Ed.* **2019**, *58*, 3285. (j) Friščić, T.; Mottillo, C.; Titi, H. M. Mechanochemistry for Synthesis. *Angew. Chem., Int. Ed.* **2020**, *59*, 1018. (k) Kubota, K.; Ito, H. Mechanochemical Cross-Coupling Reactions. *Trends Chem.* **2020**, *2*, 1066. (l) Ardila-Fierro, K. J.; Hernández, J. G. Sustainability Assessment of Mechanochemistry by Using the Twelve Principles of Green Chemistry. *ChemSusChem* **2021**, *14*, 2145. (m) Bolt, R. R. A.; Leitch, J. A.; Jones, A. C.; Nicholson, W. I.; Browne, D. L. Continuous flow mechanochemistry: reactive extrusion as an enabling technology in organic synthesis. *Chem. Soc. Rev.* **2022**, *51*, 4243. (n) Cuccu, F.; De Luca, L.; Delogu, F.; Colacino, E.; Solin, N.; Mocci, R.; Porcheddu, A. Mechanochemistry: New Tools to Navigate the Uncharted Territory of "Impossible" Reactions. *ChemSusChem* **2022**, *15*, e202200362. (o) Williams, M. T. J.; Morrill, L. C.; Browne, D. L. Mechanochemical Organocatalysis: Do High Enantioselectivities Contradict What We Might Expect?. *ChemSusChem* **2022**, *15*, e202102157. (p) Hwang, S.; Grätz, S.; Borchardt, L. A guide to direct mechanocatalysis. *Chem. Commun.* **2022**, *58*, 1661.

(20) Recent examples of mechanochemical organic synthesis utilizing inert bulk metals and inorganic salts: (a) Kubota, K.; Pang, Y.; Miura, A.; Ito, H. Redox reactions of small organic molecules using ball milling and piezoelectric materials. *Science* **2019**, *366*, 1500. (b) Takahashi, R.; Hu, A.; Gao, P.; Pang, Y.; Seo, T.; Jiang, J.; Maeda, S.; Takaya, H.; Kubota, K.; Ito, H. Mechanochemical synthesis of magnesium-based carbon nucleophiles in air and their use in organic synthesis. *Nat. Commun.* **2021**, *12*, 6691. (c) Gao, P.; Jiang, J.; Maeda, S.; Kubota, K.; Ito, H. Mechanochemically Generated Calcium-Based Heavy Grignard Reagents and Their Application to Carbon−Carbon Bond-Forming Reaction. *Angew. Chem., Int. Ed.* **2022**, *61*, e202207118. (d) Takahashi, R.; Gao, P.; Kubota, K.; Ito, H. Mechanochemical protocol facilitates the generation of arylmanganese nucleophiles from unactivated manganese metal. *Chem. Sci.* **2023**, *14*, 499. (e) Jones, A. C.; Leitch, J. A.; Raby-Buck, S. E.; Browne, D. L. Mechanochemical techniques for the activation and use of zero-valent metals in synthesis. *Nat. Synth.* **2022**, *1*, 763.

(21) Liquid-assisted grinding: (a) Friščić, T.; Trask, A. V.; Jones, W.; Motherwell, W. D. S. Screening for Inclusion Compounds and Systematic Construction of Three-Component Solids by Liquid-Assisted Grinding. *Angew. Chem., Int. Ed.* **2006**, *45*, 7546. (b) Friščić, T.; Trask, A. V.; Motherwell, W. D. S.; Jones, W. Guest-Directed Assembly of Caffeine and Succinic Acid into Topologically Different Heteromolecular Host Networks upon Grinding. *Cryst. Growth Des.* **2008**, *8*, 1605. (c) Friščić, T.; Childs, S. L.; Rizvi, S. A. A.; Jones, W. The role of solvent in mechanochemical and sonochemical cocrystal formation: a solubility-based approach for predicting cocrystallisation outcome. *CrystEngComm* **2009**, *11*, 418. Also see ref 19j.

(22) Reactivity and instability in *bay*-region of PAHs: (a) Sahara, K.; Abe, M.; Zipse, H.; Kubo, T. Duality of Reactivity of a Biradicaloid Compound with an *o*-Quinodimethane Scaffold. *J. Am. Chem. Soc.* **2020**, *142*, 5408. (c) See ref 16b for the examples of *bay*-region selective annulative π-extension reaction of PAHs.

(23) The inner-vessel temperature was determined using the reaction temperature. The heat-gun preset, reaction vessel surface, and inner vessel temperatures were measured using a thermographic camera. For details, see SI.

(24) Complexes of Li^+ and PAH anions: (a) Zhou, Z.; Zhu, Y.; Wei, Z.; Bergner, J.; Neiß, C.; Doloczki, S.; Görling, A.; Kivala, M.; Petrukhina, M. A. Reduction of π-Expanded Cyclooctatetraene with Lithium: Stabilization of the Tetra-Anion through Internal Li+ Coordination. *Angew. Chem., Int. Ed.* **2021**, *60*, 3510. (b) Eisenberg, D.; Quimby, J. M.; Jackson, E. A.; Scott, L. T.; Shenhar, R. Highly charged supramolecular oligomers based on the dimerization of corannulene tetraanion. *Chem. Commun.* **2010**, *46*, 9010.

(25) The Gaussian key word "guess(mix,always)" was used for the calculations of open-shell symmetry-broken singlet dianion state. Also see ref 13f.

(26) (a) Becke, A. D. Density-functional thermochemistry. III. The role of exact exchange. *J. Chem. Phys.* **1993**, *98*, 5648-5652. (b) Lee, C.; Yang, W.; Parr, R. G. Development of the Colle-Salvetti correlation-energy formula into a functional of the electron density. *Phys. Rev. B* **1988**, *37*, 785-789. (c) Tomasi, J.; Mennucci, B.; Cammi, R. Quantum Mechanical Continuum Solvation Models. *Chem. Rev.* **2005**, *105*, 2999.

(27) Frisch, M. J.; Trucks, G. W.; Schlegel, H. B.; Scuseria, G. E.; Robb, M. A.; Cheeseman, J. R.; Scalmani, G.; Barone, V.; Petersson, G. A.; Nakatsuji, H.; Li, X.; Caricato, M.; Marenich, A. V.; Bloino, J.; Janesko, B. G.; Gomperts, R.; Mennucci, B.; Hratchian, H. P.; Ortiz, J. V.; Izmaylov, A. F.; Sonnenberg, J. L.; Williams; Ding, F.; Lipparini, F.; Egidi, F.; Goings, J.; Peng, B.; Petrone, A.; Henderson, T.; Ranasinghe, D.; Zakrzewski, V. G.; Gao, J.; Rega, N.; Zheng, G.; Liang, W.; Hada, M.; Ehara, M.; Toyota, K.; Fukuda, R.; Hasegawa, J.; Ishida, M.; Nakajima, T.; Honda, Y.; Kitao, O.; Nakai, H.; Vreven, T.; Throssell, K.; Montgomery Jr., J. A.; Peralta, J. E.; Ogliaro, F.; Bearpark, M. J.; Heyd, J. J.; Brothers, E. N.; Kudin, K. N.; Staroverov, V. N.; Keith, T. A.; Kobayashi, R.; Normand, J.; Raghavachari, K.; Rendell, A. P.; Burant, J. C.; Iyengar, S. S.; Tomasi, J.; Cossi, M.; Millam, J. M.; Klene, M.; Adamo, C.; Cammi, R.; Ochterski, J. W.; Martin, R. L.; Morokuma, K.; Farkas, O.; Foresman, J. B.; Fox, D. J. *Gaussian 16 Rev. C.01*, Wallingford, CT, **2016**.

(28) NCI plot analysis by a NCIPLOT program ver. 4.0: (a) Johnson, E. R.; Keinan, S.; Mori-Sánchez, P.; Contreras-García, J.; Cohen, A. J.; Yang, W. Revealing Noncovalent Interactions. *J. Am. Chem. Soc.* **2010**, *132*, 6498. (b) Contreras-García, J.; Johnson, E. R.; Keinan, S.; Chaudret, R.; Piquemal, J.-P.; Beratan, D. N.; Yang, W. NCIPLOT: A Program for Plotting Noncovalent Interaction Regions. *J. Chem. Theory Comput.* **2011**, *7*, 625. (c) Boto, R. A.; Peccati, F.; Laplaza, R.; Quan, C.; Carbone, A.; Piquemal, J.-P.; Maday, Y.; Contreras-García, J. NCIPLOT4: Fast, Robust, and Quantitative Analysis of Noncovalent Interactions. *J. Chem. Theory Comput.* **2020**, *16*, 4150.

(29) (a) Laarhoven, W. H.; van Broekhoven, J. A. M. Synthesis and spectral properties of tribenzo[*c,i,o*]triphenylene and its anions. *Tetrahedron Lett.* **1970**, *11*, 73. (b) Hagen, S.; Scott, L. T. A Convenient Synthesis of Benzo[*c*]naphtho[2,1-*p*]chrysene. *J. Org. Chem.* **1996**, *61*, 7198. (c) Hagen, S.; Bratcher, M. S.; Erickson, M. S.; Zimmermann, G.; Scott, L. T. Novel Syntheses of Three $C_{30}H_{12}$ Bowl-Shaped Polycyclic Aromatic Hydrocarbons. *Angew. Chem., Int. Ed.* **1997**, *36*, 406. (d) Peña, D.; Pérez, D.; Guitián, E.; Castedo, L. Synthesis of Hexabenzotriphenylene and Other Strained Polycyclic Aromatic Hydrocarbons by Palladium-Catalyzed Cyclotrimerization of Arynes. *Org. Lett.* **1999**, *1*, 1555.

(30) Nomenclatures of "perylene", "terylene" and "quaterrylene" having Latin prefixes have been classically and widely used to express shorter [*n*]rylenes (*n*: number of naphthalene units). However, recent synthetic and theoretical reports on [*n*]rylene ($n \geqq 5$) use inconsistent nomenclatures like pentarylene ($n = 5$), hexarylene ($n = 6$), heptarylene ($n = 7$), octarylene ($n = 8$) and nonarylene ($n = 9$) having Greek prefixes. Here, we recommend to use consistent prefixes for expressing rylenes such as quinterrylene ([5]rylene),

sexterrylene ([6]rylene), septimerrylene ([7]rylene), oxtaverrylene ([8]rylene). For longer rylenes than oxtaverrylene, it is better to use [*n*]rylene for clarity.

(31) Markiewicz, J. T.; Wudl, F. Perylene, Oligorylenes, and Aza-Analogs. *ACS Appl. Mater. Interfaces* **2015**, *7*, 28063.

(32) Rylene: (a) Karabunarliev, S.; Baumgarten, M.; Mullen, K. Crossover to an Even-Parity Lowest Excited Singlet in Large Oligorylenes: A Theoretical Study. *J. Phys. Chem. A* **1998**, *102*, 7029. (b) Viruela-Martin, R.; Viruela-Martin, P. M.; Orti, E. Viruela-Martin, R.; Viruela-Martin, P. M.; Orti, E. Theoretical determination of the geometric and electronic structures of oligorylenes and poli(*peri*-naphthalene). *J. Chem. Phys.* **1992**, *97*, 8470. (c) Bakhshi, A. K.; Ladik, J. On the observed high conductivity of poly(perinaphthalene) chains. *Synth. Met.* **1989**, *30*, 115. (d) Tanaka, K.; Ueda, K.; Koike, T.; Yamabe, T. Electronic structure of polyperylene. *Solid State Commun.* **1984**, *51*, 943. (e) Minami, T.; Ito, S.; Nakano, M. Diradical Character View of Singlet Fission. *J. Phys. Chem. Lett.* **2012**, *3*, 2719. (f) Avlasevich, Y.; Kohl, C.; Müllen, K. Facile synthesis of terrylene and its isomer benzoindenoperylene. *J. Mater. Chem.* **2006**, *16*, 1053.

(33) Graphene nanoribbon with $N = 5$ of width: (a) Sakaguchi, H.; Kawagoe, Y.; Hirano, Y.; Iruka, T.; Yano, M.; Nakae, T. Width-Controlled Sub-Nanometer Graphene Nanoribbon Films Synthesized by Radical-Polymerized Chemical Vapor Deposition. *Adv. Mater.* **2014**, *26*, 4134. (b) Kimouche, A.; Ervasti, M. M.; Drost, R.; Halonen, S.; Harju, A.; Joensuu, P. M.; Sainio, J.; Liljeroth, P. Ultra-narrow metallic armchair graphene nanoribbons. *Nat. Commun.* **2015**, *6*, 10177. (c) Chen, Z. P.; Wang, H. I.; Bilbao, N.; Teyssandier, J.; Prechtl, T.; Cavani, N.; Tries, A.; Biagi, R.; De Renzi, V.; Feng, X. L.; Klaui, M.; De Feyter, S.; Bonn, M.; Narita, A.; Müllen, K. Lateral Fusion of Chemical Vapor Deposited $N = 5$ Armchair Graphene Nanoribbons. *J. Am. Chem. Soc.* **2017**, *139*, 9483. (d) Kitao, T.; MacLean, M. W. A.; Nakata, K.; Takayanagi, M.; Nagaoka, M.; Uemura, T. Scalable and Precise Synthesis of Armchair-Edge Graphene Nanoribbon in Metal–Organic Framework. *J. Am. Chem. Soc.* **2020**, *142*, 5509. (e) Vandescuren, M.; Hermet, P.; Meunier, V.; Henrard, L.; Lambin, P. Theoretical study of the vibrational edge modes in graphene nanoribbons. *Phys. Rev. B.* **2008**, *78*, 195401. (f) Zhou, J.; Dong, J. Vibrational property and Raman spectrum of carbon nanoribbon. *Appl. Phys. Lett.* **2007**, *91*, 173108.

(34) Quaterrylene: (a) Clar, E. Oligomers of peri-condensed naphthylenes have been termed "rylenes." *Chem. Ber.* **1948**, *81*, 52. (b) Cataldo, F.; Ursini, O.; Angelini, G.; Iglesias-Groth, S. *Fullerenes, Nanotubes, Carbon Nanostruct* **2011**, *19*, 713. (c) Thanmatam, R.; Skraba, S. L.; Johnson, R. P. Scalable synthesis of quaterrylene: solution-phase ^{1}H NMR spectroscopy of its oxidative dication. *Chem. Commun.* **2013**, *49*, 9122. (d) Bohnen, A.; Koch, K. H.; Luettke W.; Müllen, K. Oligorylene as a Model for "Poly(perinaphthalene)". *Angew. Chem., Int. Ed.* **1990**, *29*, 525.

(35) Kesharwani, M. K.; Bauer, B.; Martin, J. M. L. Frequency and zero-point vibrational energy scale factors for double-hybrid density functionals (and Other Selected Methods): Can Anharmonic Force Fields Be Avoided?. *J. Phys. Chem. A* **2015**, *119*, 1701.

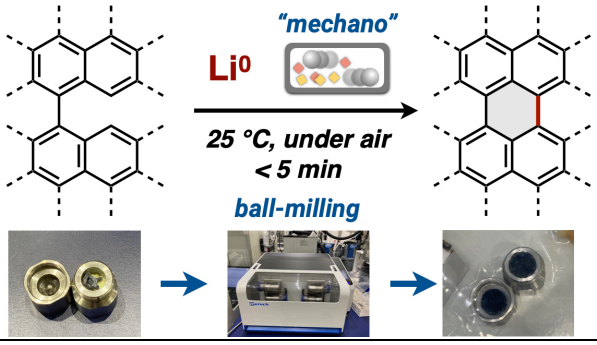
"mechano"
Li0
25 °C, under air
< 5 min
ball-milling